ARTICLES

Mixed Quantum and Forward−Backward Semiclassical Dynamics†

Ed Bukhman and Nancy Makri*

Department of Chemistry, University of Illinois, Urbana, Illinois 61801

Received: November 4, 2008; Revised Manuscript Received: January 26, 2009

Forward−backward semiclassical dynamics (FBSD) has been shown to offer quantitative descriptions of the short time dynamics of low-temperature fluids. This article aims to correct the major shortcoming of FBSD, namely, its inability to capture dynamical effects of a purely quantum mechanical nature such as tunneling. To this end, we extend the methodology to a quantum-FBSD scheme, where the evolution along the coordinates of a quantum particle is obtained by quantum propagation subject to a time-dependent potential that is evaluated along classical trajectories describing the solvent, whose phase space distributions are determined by FBSD relations. Numerical tests on a dissipative two-level system show that the quantum-FBSD methodology offers a semiquantitative description of the quenched tunneling oscillations. Therefore, the quantum-FBSD methodology will prove to be useful for simulating the dynamics of proton and electron transfer in condensed phase and biological environments.

I. Introduction

As is well known, the nonlocal nature of quantum mechanics leads to an exponential scaling of required computational power with the number of coupled degrees of freedom. As a result, direct solution of the Schrödinger equation is feasible for systems with a moderate number of electrons or atoms but is computationally prohibitive when the number of interacting particles is large. Available alternatives, such as the path integral formulation of time-dependent quantum mechanics, require the evaluation of high-dimensional integrals of oscillatory functions. Stochastic sampling methods,[1] which are ideally suited for multidimensional integration of functions that are localized and smooth, fail to converge in polynomial computer time when the integrand is highly oscillatory, and thus numerical evaluation of the path integral presents a major challenge.[2] Iterative path integral methods[3−7] circumvent this difficulty and allow numerically exact calculation of the dynamics in system−bath models. However, despite its utility and relevance for many important problems, the system−bath Hamiltonian[8] does not provide an adequate treatment of the dynamics of fluids and of many biological processes. Therefore, there is currently much interest in approximate simulation methods that are applicable to processes in complex many-particle systems. Several of such methods have been developed in the last two decades, including centroid molecular dynamics,[9,10] quantum mode coupling theory,[11] maximum entropy ideas for the inversion of imaginary-time data,[12,13] ring polymer dynamics,[14,15] and approaches based on the time-dependent semiclassical approximation,[16] which can be broadly classified as fully semiclassical techniques[17−19] (which preserve the phase that gives rise to quantum interference) and quasiclassical methods, such as the Wigner model[20] (also derived by linearizing the semiclassical expression[21] or the path integral expression[22]) and forward−backward semiclassical dynamics (FBSD).[23−32] Unfortunately, assessing the accuracy of these approximate methods in realistic systems presents a difficult task. Some progress in this direction was recently reported.[33,34] In addition, a new iterative Monte Carlo path integral methodology applicable to general Hamiltonians allows propagation to long times and thus appears to be promising.[35]

A series of papers by our group have presented an FBSD approximation to time correlation functions on the basis of an exponential derivative identity,[26,27,36] its numerical implementation and properties,[37−45] and various applications to fluids.[28,46−50] This methodology for evaluating time correlation functions constitutes a rigorous stationary phase limit of the full quantum mechanical expression. The FBSD integrand obtains dynamical information from classical trajectories and is free of the oscillatory semiclassical phase, allowing convergence in simulations with hundreds of degrees of freedom. Full quantization of the Boltzmann density operator is possible, and thus the zero time value of the FBSD correlation function converges to the exact quantum mechanical result. A number of calculations on fluids,[28,47−50] including a simulation of helium across the lambda transition[50] and recent comparison with accurate quantum mechanical results,[33,34] have demonstrated that FBSD provides an accurate description of the early time dynamics in low-temperature fluids where quantum mechanical (and in some cases quantum statistical) effects are dominant.

The limitations of FBSD arise precisely from those features that make it so versatile and efficient, namely, the elimination of the semiclassical phase and the use of classical trajectories. As a result, FBSD cannot capture quantum coherence or tunneling effects during the course of time evolution.[19,26] Whereas coherence is naturally quenched in most condensed phase processes and tunneling is not expected to be significant in the dynamics of neat fluids, the incorporation of such effects is a necessary step for applying the FBSD methodology to the dynamics of a quantum mechanical subsystem (electron, proton,

† Part of the special issue "Robert Benny Gerber Festschrift".

* Corresponding author.

10.1021/jp809741x CCC: $40.75
Published on Web 03/24/2009

or small molecule) in solution. We recently reported some progress toward treating such systems,[44] focusing on convergence issues of FBSD. The present article is concerned with the more severe limitation associated with the extraction of dynamical information based on laws of classical mechanics. To allow for an accurate description of quantum mechanical effects for the small subsystem of interest, we present a quantum-FBSD methodology in which the dynamics of the quantum subsystem is treated fully quantum mechanically and that of the solvent is treated by FBSD, coupling the two descriptions by a mixed quantum-classical approximation.[51,52] We also describe a multiconfiguration extension of the quantum-classical approximation in the spirit of the (fully quantum mechanical) multiconfiguration time-dependent self-consistent field approximation, which further improves the accuracy of the propagation. The quantum-FBSD methodology is similar in spirit to earlier quantum-semiclassical treatments on the basis of linearization of the solvent forward−backward action,[24,25,53−55] but the present formalism differs substantially from these methods.

The quantum-FBSD methodology is presented in Section II, along with single- and multiconfiguration quantum-classical treatment we employ for the time evolution. Illustrative applications to the dynamics of a two-level system (TLS) in a bath of harmonic oscillators are shown in Section III. Finally, some concluding remarks are given in Section IV.

II. Methodology

The central feature of the scheme we lay out in this article is the extension of the FBSD methodology to allow a fully quantum mechanical treatment of a small molecular system in contact with a solvent. The starting point is the molecule−solvent partitioning we adopted in our previous paper[44]

$$\hat{H} = H_{\mathrm{mol}}(\hat{r},\hat{p}) + H_{\mathrm{sol}}(\hat{\mathbf{R}},\hat{\mathbf{P}}) + V(\hat{r},\hat{\mathbf{R}}) \tag{2.1}$$

where r denotes the coordinate(s) of the system of interest (an electron, atom, or small molecule), the d-dimensional vector $\mathbf{R}$ contains the Cartesian coordinates of the solvent atoms (the bath), and $V(r,\mathbf{R})$ is the potential coupling function. We use 1D notation for the system coordinate for notational clarity.

We consider a time correlation function, given by the expression

$$C_{\mathbf{A}\cdot\mathbf{B}}(t) = \mathrm{Tr}(\hat{\rho}_0\hat{\mathbf{A}}(0)\cdot\hat{\mathbf{B}}(t)) = \mathrm{Tr}(\hat{\rho}_0\hat{\mathbf{A}}\cdot \mathrm{e}^{i\hat{H}t/\hbar}\hat{\mathbf{B}}\mathrm{e}^{-i\hat{H}t/\hbar}) \tag{2.2}$$

where $\hat{\rho}_0$ is the operator describing the initial density, $\hat{\mathbf{A}}$ and $\hat{\mathbf{B}}$ are vectors denoting the operators of interest, and the trace is over all degrees of freedom. For clarity of presentation, we indicate the system and bath components of the probed operators as $A_{\mathrm{mol}}(\hat{r},\hat{p})$, $\mathbf{A}_{\mathrm{sol}}(\hat{\mathbf{R}},\hat{\mathbf{P}})$ and $B_{\mathrm{mol}}(\hat{r},\hat{p})$, $\mathbf{B}_{\mathrm{sol}}(\hat{\mathbf{R}},\hat{\mathbf{P}})$. For example, the choice $\hat{A}_{\mathrm{mol}} = \hat{B}_{\mathrm{mol}} = \hat{p}$, $\hat{A}_{\mathrm{sol}} = \hat{B}_{\mathrm{sol}} = \hat{\mathbf{P}}$ gives the momentum autocorrelation function of all particles, whereas the choice $\hat{A}_{\mathrm{mol}} = \hat{B}_{\mathrm{mol}} = \hat{x}$, $\hat{A}_{\mathrm{sol}} = \hat{B}_{\mathrm{sol}} = 1$ produces the position autocorrelation function of the molecule of interest in contact with the solvent. We note, however, that the operators of interest need not have such simple forms; a generalization of the quantum-FBSD treatment is given later in this section.

We propagate the molecular and solvent parts within a time-dependent self-consistent field (TDSCF) model,[56−61] approximating the time evolution operator $\hat{U}(t)$ by a product of operators that act in the two subspaces

$$\hat{U}_{\mathrm{mol}}(t)\hat{U}_{\mathrm{sol}}(t) \tag{2.3}$$

The interaction between solute and solvent takes place through the interdependence of these evolution operators. The first factor in eq 2.3 describes time evolution under a system Hamiltonian that is time-dependent by virtue of the mean field potential arising from the molecule−solvent interaction. Similarly, the time evolution operator for the solvent also corresponds to a time-dependent mean field Hamiltonian that depends on the dynamics of the molecular system. For simplicity, we consider first a separable initial condition,[62] where the density operator factorizes into system and bath components

$$\hat{\rho}_0 = \hat{\rho}_{\mathrm{mol}}(0)\hat{\rho}_{\mathrm{sol}}(0) \tag{2.4}$$

Equation 2.4 is often a reasonable approximation for the calculation of expectation values ($\hat{A} = 1$). In that case, and with the assumptions given in the last two expressions, eq 2.2 becomes a product of time-dependent factors for the molecular and solvent parts, whose evolution is to be calculated self-consistently within a mean field approximation

$$C_{\mathbf{A}\cdot\mathbf{B}}(t) = \mathrm{Tr}_{\mathrm{mol}}(\hat{\rho}_{\mathrm{mol}}\hat{A}_{\mathrm{mol}}\hat{\mathrm{U}}^{\dagger}_{\mathrm{mol}}(t)\hat{B}_{\mathrm{mol}}\hat{U}_{\mathrm{mol}}(t)) \times \mathrm{Tr}_{\mathrm{sol}}(\hat{\rho}_{\mathrm{sol}}\hat{\mathrm{A}}_{\mathrm{sol}}\hat{\mathrm{U}}^{\dagger}_{\mathrm{sol}}(t)\hat{\mathrm{B}}_{\mathrm{sol}}\hat{U}_{\mathrm{sol}}(t)) \tag{2.5}$$

Our goal is to calculate the molecular part by a fully quantum mechanical method, whereas the solvent will be treated within the FBSD approximation.

In general, the factorized initial condition for the density operator, eq 2.4, is not valid. In particular, in the calculation of time correlation functions at finite temperature, the initial density is given by the Boltzmann operator

$$\hat{\rho}_0 = \frac{\mathrm{e}^{-\beta\hat{H}}}{Z} \tag{2.6}$$

where $\beta = 1/k_{\mathrm{B}}T$ and Z is the canonical partition function. By evaluating the trace with respect to the system and making use again of the TDSCF factorization of the time evolution operator, the correlation function is written as

$$C_{\mathbf{A}\cdot\mathbf{B}}(t) = Z^{-1}\int \mathrm{d}\mathbf{R}_0 \int \mathrm{d}\mathbf{R}_N \int \mathrm{d}r_0 \int \mathrm{d}r_N \langle r_N|\langle \mathbf{R}_N|\mathrm{e}^{-\beta\hat{H}}|\mathbf{R}_0\rangle|r_0\rangle \times \langle \mathbf{R}_0|\hat{\mathrm{A}}_{\mathrm{sol}}\cdot\hat{\mathrm{U}}^{\dagger}_{\mathrm{sol}}(t)\hat{\mathrm{B}}_{\mathrm{sol}}\hat{U}_{\mathrm{sol}}(t)|\mathbf{R}_N\rangle\langle r_0|\hat{A}_{\mathrm{mol}}\hat{\mathrm{U}}^{\dagger}_{\mathrm{mol}}(t)\hat{B}_{\mathrm{mol}}\hat{U}_{\mathrm{mol}}(t)|r_N\rangle \tag{2.7}$$

Use of the discretized path integral[63−65] representation of the Boltzmann operator with $\Delta\beta = \beta/N$ gives

$$C_{\mathbf{A}\cdot\mathbf{B}}(t) = Z^{-1}\int d\mathbf{r}_0\int d\mathbf{r}_1...\int d\mathbf{r}_N\int d\mathbf{R}_0\int d\mathbf{R}_1...\int d\mathbf{R}_N \times e^{-\Delta\beta V(\mathbf{R}_N,r_N)}\langle\mathbf{R}_N|e^{-\frac{1}{2}\Delta\beta\hat{H}_{sol}}|\mathbf{R}_{N-1}\rangle\langle r_N|e^{-\frac{1}{2}\Delta\beta\hat{H}_{mol}}|r_{N-1}\rangle... \times e^{-\Delta\beta V(\mathbf{R}_2,r_2)}\langle\mathbf{R}_2|e^{-\Delta\beta\hat{H}_{sol}}|\mathbf{R}_1\rangle\langle r_2|e^{-\Delta\beta\hat{H}_{mol}}|r_1\rangle \times e^{-\Delta\beta V(\mathbf{R}_1,r_1)}\langle\mathbf{R}_1|e^{-\frac{1}{2}\Delta\beta\hat{H}_{sol}}|\mathbf{R}_0\rangle\langle r_1|e^{-\frac{1}{2}\Delta\beta\hat{H}_{mol}}|r_0\rangle \times \langle\mathbf{R}_0|\hat{\mathbf{A}}_{sol}\cdot\hat{\mathbf{U}}^{\dagger}_{sol}(t)\hat{\mathbf{B}}_{sol}\hat{U}_{sol}(t)|\mathbf{R}_N\rangle\langle r_0|\hat{A}_{mol}\hat{U}^{\dagger}_{mol}(t)\hat{B}_{mol}\hat{U}_{mol}(t)|r_N\rangle \quad (2.8)$$

Finally, collecting the factors that depend on molecular coordinates, we obtain

$$C_{\mathbf{A}\cdot\mathbf{B}}(t) = Z^{-1}\int d\mathbf{R}_0\int d\mathbf{R}_1...\int d\mathbf{R}_N\langle\mathbf{R}_N|e^{-\frac{1}{2}\Delta\beta\hat{H}_{sol}}|\mathbf{R}_{N-1}\rangle... \langle\mathbf{R}_2|e^{-\Delta\beta\hat{H}_{sol}}|\mathbf{R}_1\rangle\langle\mathbf{R}_1|e^{-\frac{1}{2}\Delta\beta\hat{H}_{sol}}|\mathbf{R}_0\rangle \times \langle\mathbf{R}_0|\hat{\mathbf{A}}_{sol}\cdot\hat{\mathbf{U}}^{\dagger}_{sol}(t)\hat{\mathbf{B}}_{sol}\hat{U}_{sol}(t)|\mathbf{R}_N\rangle C_{mol}(\mathbf{R}_1,...,\mathbf{R}_N;t) \quad (2.9)$$

where

$$C_{mol}(\mathbf{R}_1,...,\mathbf{R}_N;t) = \mathrm{Tr}_{mol}\Big(e^{-\Delta\beta V(\mathbf{R}_N,\hat{r})}e^{-\frac{1}{2}\Delta\beta\hat{H}_{mol}}...e^{-\Delta\beta V(\mathbf{R}_2,\hat{r})} \times e^{-\Delta\beta\hat{H}_{mol}}e^{-\Delta\beta V(\mathbf{R}_1,\hat{r})}e^{-\frac{1}{2}\Delta\beta\hat{H}_{mol}}\hat{A}_{mol}\hat{U}^{\dagger}_{mol}(t)\hat{B}_{mol}\hat{U}_{mol}(t)\Big) \quad (2.10)$$

is the time correlation function of the molecular system with respect to an imaginary-time-dependent Hamiltonian generated by the interaction with the solvent.

The solvent part of eq 2.9 is itself reminiscent of a time correlation function. To see this, we rewrite eq 2.9 in the form

$$C_{\mathbf{A}\cdot\mathbf{B}}(t) = \mathrm{Tr}(\hat{q}_N e^{-\frac{1}{2}\Delta\beta\hat{H}_{sol}}\hat{q}_{N-1}...e^{-\Delta\beta\hat{H}_{sol}} \times \hat{q}_1 e^{-\frac{1}{2}\Delta\beta\hat{H}_{sol}}\hat{\mathbf{A}}_{sol}\cdot\hat{\mathbf{U}}^{\dagger}_{sol}(t)\hat{\mathbf{B}}_{sol}\hat{U}_{sol}(t)) \equiv \mathrm{Tr}(\tilde{\rho}_0\hat{\mathbf{A}}_{sol}\cdot\hat{\mathbf{U}}^{\dagger}_{sol}(t)\hat{\mathbf{B}}_{sol}\hat{U}_{sol}(t)) \quad (2.11)$$

where $\hat{q}_1, ..., \hat{q}_N$ are time- and solvent coordinate-dependent operators that produce eq 2.10 when evaluated in the position representation, and the density $\tilde{\rho}_0$ is defined accordingly. Therefore, we apply the FBSD approximation to eq 2.9[26,27] with the discretized path integral representation of the Boltzmann density.[36] This procedure involves replacement of the integral over $\mathbf{R}_0$ by a phase space integral. Introducing coherent state functions $|\mathbf{R}_0\mathbf{P}_0\rangle$, defined by the relation[66]

$$\langle\mathbf{R}|\mathbf{R}_0\mathbf{P}_0\rangle = \left(\frac{2}{\pi}\right)^{d/4}(\det\gamma)^{1/4}\exp\Big[-(\mathbf{R}-\mathbf{R}_0)\cdot\gamma\cdot(\mathbf{R}-\mathbf{R}_0) + \frac{i}{\hbar}\mathbf{P}_0\cdot(\mathbf{R}-\mathbf{R}_0)\Big] \quad (2.12)$$

and assuming that the operators of interest are of polynomial form, the correlation function in the quantum-classical approximation to the molecule−solvent dynamics becomes

$$C_{\mathbf{A}\cdot\mathbf{B}}(t) = (2\pi\hbar)^{-d}\int d\mathbf{R}_0\int d\mathbf{P}_0\int d\mathbf{R}_1... \int d\mathbf{R}_N\langle\mathbf{R}_0\mathbf{P}_0|e^{-\frac{1}{2}\Delta\beta\hat{H}_{sol}}|\mathbf{R}_N\rangle...\langle\mathbf{R}_2|e^{-\Delta\beta\hat{H}_{sol}}|\mathbf{R}_1\rangle \times \langle\mathbf{R}_1|e^{-\frac{1}{2}\Delta\beta\hat{H}_{sol}}|\mathbf{R}_0\mathbf{P}_0\rangle\Lambda_{\mathbf{A}_{sol}\cdot\mathbf{B}_{sol}}(\mathbf{R}_0,\mathbf{P}_0,\mathbf{R}_1,...,\mathbf{R}_N;t) \times C_{mol}(\mathbf{R}_0,\mathbf{R}_1,...,\mathbf{R}_N;t) \quad (2.13)$$

Here the dynamics of the solvent is described by a swarm of classical trajectories launched from points $\mathbf{R}_0$ and $\mathbf{P}_0$, which at the time, t, have phase space coordinates $\mathbf{R}_t$ and $\mathbf{P}_t$, and $\Lambda_{\mathbf{A}_{sol}\cdot\mathbf{B}_{sol}}$ is a factor that depends on $\mathbf{B}_{sol}(\mathbf{R}_t,\mathbf{P}_t)$. The molecular part of eq 2.13 is to be evaluated by a fully quantum mechanical propagation method along a time-dependent Hamiltonian evaluated at the instantaneous coordinate of the given solvent trajectory. Because of the time-dependent mean field approximation, the Hamiltonian that generates the dynamics of the solvent trajectories is itself time-dependent. Therefore, for each solvent trajectory, the molecule−solvent dynamics follows a quantum-classical version of the TDSCF approximation.[51,52]

In previous implementations of quantum-classical propagation approximations, the initial conditions of the trajectories were given by the classical Boltzmann factor or, in simple cases, by the Wigner transform of the quantum density operator. The Wigner phase space density offers an excellent way of accounting for zero-point energy (or quantum dispersion) fluctuations of the solvent, but performing the necessary integrals to obtain the Wigner function for a many-particles solvent governed by anharmonic intermolecular interactions is in itself an extremely difficult task. Some recent efforts to approximate the Wigner density[32,67,68] have achieved considerable success. The present FBSD treatment involves a phase space density given by coherent state matrix elements of a quantum mechanical operator. These can be straightforwardly evaluated using the imaginary-time path integral method.

Finally, it is convenient to evaluate the trace of the system correlation function in a discrete basis set rather than in the basis of coordinate states. Therefore, we rewrite eq 2.10 in the form

$$C_{mol}(\mathbf{R}_1,...,\mathbf{R}_N;t) = \sum_n\langle\phi_n|e^{-\Delta\beta V(\mathbf{R}_N,\hat{r})}e^{-\frac{1}{2}\Delta\beta\hat{H}_{mol}}... e^{-\Delta\beta V(\mathbf{R}_2,\hat{r})}e^{-\Delta\beta\hat{H}_{mol}}e^{-\Delta\beta V(\mathbf{R}_1,\hat{r})}e^{-\frac{1}{2}\Delta\beta\hat{H}_{mol}} \times \hat{A}_{mol}\hat{U}^{\dagger}_{mol}[\mathbf{R}(t')]\hat{B}_{mol}\hat{U}_{mol}[\mathbf{R}(t')]|\phi_n\rangle \quad (2.14)$$

where $\hat{U}_{mol}[\mathbf{R}(t')]$ is the time evolution operator for the molecular system in the time-dependent field of the solvent along the classical trajectory $\mathbf{R}(t')$ $(0 \le t' \le t)$.

It is now easy to generalize the quantum-FBSD treatment to arbitrary operators by allowing $\hat{A}_{mol}$ and $\hat{B}_{mol}$ to depend on the solvent coordinates as well. With the replacement $\hat{\mathbf{R}} \rightarrow \mathbf{R}(t)$, $\hat{\mathbf{P}} \rightarrow \hat{\mathbf{P}}(t)$, eq 2.14 remains unchanged, but now the probed operators are evaluated with the solvent coordinates set to the values of the corresponding classical trajectory.

Equation 2.13, together with eq 2.14 (which is to be evaluated by wave function propagation methods), constitute a mixed quantum-FBSD treatment of the molecule−solvent dynamics. We note that the mean field equations are nonlinear; consequently, the evolution depends on the initial conditions (and thus on the choice of basis functions). Below we describe single- and two-configuration quantum-classical propagation approximations.

a. Single-Configuration Approximation. This follows the standard quantum-classical approximation[51,52] in which the evolution of the wave function

$$|\psi_n(t)\rangle \equiv \hat{U}_{\mathrm{mol}}[\mathbf{R}_n(t')]|\psi_n(0)\rangle \tag{2.15}$$

(where $|\psi_n(0)\rangle = |\phi_n\rangle$) is given by the Schrödinger equation with a time-dependent potential determined by the instantaneous position of the solvent particles along a particular trajectory

$$i\hbar\frac{\partial}{\partial t'}|\psi_n(t')\rangle = \{\hat{H}_{\mathrm{mol}} + V(\hat{r}, \mathbf{R}_n(t'))\}|\psi_n(t')\rangle \tag{2.16}$$

while each solvent trajectory follows the equation of motion

$$m\ddot{\mathbf{R}}_n(t') = -\frac{\partial}{\partial \mathbf{R}_n(t')}\{H_{\mathrm{sol}}(\mathbf{R}_n(t'), \mathbf{P}_n(t')) + \langle\varphi_k|V(\hat{r}, \mathbf{R}_{nk}(t'))|\varphi_k\rangle\} \tag{2.17}$$

Note that because the Hamiltonian in eq 2.16 is hermitian, the norm of the wave function is preserved. Equations 2.16 and 2.17 are solved self-consistently for each system basis function and solvent trajectory.

b. Two-Configuration Approximation. The single-configuration version of the time-dependent self-consistent field approximation fails to describe processes that involve bifurcation of the evolving wave function, necessitating multiconfiguration treatments. For example, it has been shown[69] that the standard single-configuration TDSCF treatment fails to capture the effects of tunneling in a symmetric double-well potential coupled to a harmonic bath. The multiconfiguration time-dependent self-consistent field scheme (MC-TDSCF)[69,70] is able to correct the shortcomings of the mean field approximation and often leads to semiquantitative results, even with a few configurations if these are chosen judiciously. As is well known, MC-TDSCF expansions converge to the full quantum mechanical solution as the number of configurations is increased.

Here we describe a quantum-classical MC-TDSCF approximation where the wave function for the quantum particle is expressed in terms of M spatially localized configurations, each of which evolves in the field generated by a solvent trajectory. The main difference from the single configuration approach is that the trajectory of the solvent now experiences the average force with respect to a localized wave function corresponding to the given configuration, as opposed to the global average over the entire system, thus providing a more detailed account of the molecule−solvent interaction. Unlike the fully quantum mechanical MC-TDSCF scheme, however, the multiconfiguration quantum-classical treatment we introduce here is not necessarily expected to converge to the exact dynamics because the quasiclassical nature of the solvent propagation causes destruction of phase coherence.

To propagate each system state ψ_n entering eq 2.14, the wave function is expressed as a linear combination of the orthogonal, localized basis functions φ_i ($i = 1, ..., M$) that constitute the relevant configurations

$$|\psi_n(t)\rangle = \sum_{k=1}^{M} a_{nk}(t)|\varphi_k\rangle \tag{2.18}$$

The expansion coefficients are propagated in time according to the differential equations

$$i\hbar\dot{a}_{nk}(t') = \sum_{l=1}^{M}\langle\varphi_k|H_{nk}|\varphi_l\rangle a_{nl}(t') \tag{2.19}$$

where

$$\hat{H}_{nk}(t') = \hat{H}_{\mathrm{mol}} + V(\hat{r}, \mathbf{R}_{nk}(t')) \tag{2.20}$$

The interaction potential in eq 2.20 is evaluated at the coordinate of a trajectory that obeys Newton's equations with a force that arises from the average system position calculated with respect to the particular configuration, that is

$$m\ddot{R}_{nk}(t') = -\frac{\partial}{\partial \mathbf{R}_{nk}(t')}\{H_{\mathrm{sol}}(\mathbf{R}_{nk}(t'), \mathbf{P}_{nk}(t')) + \langle\varphi_k|V(\hat{r}, \mathbf{R}_{nk}(t'))|\varphi_k\rangle\} \tag{2.21}$$

III. Applications

We illustrate the quantum-FBSD methodology on a TLS coupled to a harmonic dissipative bath. The Hamiltonian is

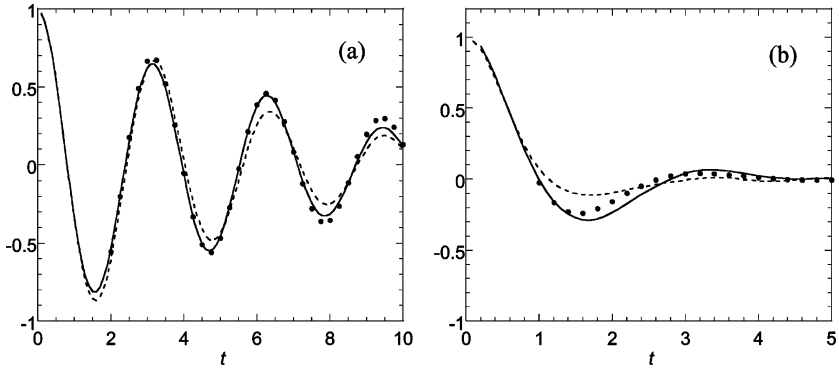

Figure 1. Average TLS position as a function of time at zero temperature for (a) $\xi = 0.09$ and (b) $\xi = 0.5675$. The bath cutoff frequency is $\omega_c = 2.5\ \Omega$. Points: exact quantum mechanical results obtained via an iterative evaluation of the path integral.[4] Dashed line: results of single-configuration quantum-FBSD calculation. Solid line: results of two-configuration quantum-FBSD calculation.

$$\hat{H}_{\mathrm{mol}} = -\hbar\Omega\hat{\sigma}_x,\ \ \hat{H}_{\mathrm{sol}} = \sum_j \frac{1}{2}\hat{\mathrm{P}}_j^2 + \frac{1}{2}m\omega_j^2\hat{\mathrm{R}}_j^2,$$
$$\hat{V} = \sum_j c_j\hat{\sigma}_z\hat{R}_j \quad (3.1)$$

where σ_x and σ_z are the Pauli spin operators, which on the basis of left- and right-localized states $|\varphi_{\mathrm{L}}\rangle$ and $|\varphi_{\mathrm{R}}\rangle$ have the form

$$\hat{\sigma}_x = |\varphi_{\mathrm{R}}\rangle\langle\varphi_{\mathrm{L}}| + |\varphi_{\mathrm{L}}\rangle\langle\varphi_{\mathrm{R}}|,\ \ \hat{\sigma}_z = |\varphi_{\mathrm{R}}\rangle\langle\varphi_{\mathrm{R}}| - |\varphi_{\mathrm{L}}\rangle\langle\varphi_{\mathrm{L}}| \quad (3.2)$$

and $2\hbar\Omega$ is the tunneling splitting. The frequencies and coupling coefficients are specified collectively by the spectral density function[62]

$$J(\omega) = \eta\omega\mathrm{e}^{-\omega/\omega_{\mathrm{c}}} \quad (3.3)$$

where the friction coefficient, η, is related to the dimensionless Kondo parameter $\xi = 2\eta/\pi\hbar$.

In the quantum-FBSD calculations, the continuous bath is approximated by a set of up to 65 harmonic oscillators. We adopt a procedure that has been previously described[71] to choose the frequencies that lead to an adequate representation of the continuous bath. The coupling constants are proportional to the frequencies.

We assume that both the TLS and bath are at zero temperature; that is, the initial density operator has the form

$$\hat{\rho}_0 = |\varphi_{\mathrm{R}}\rangle\langle\varphi_{\mathrm{R}}|\prod_j |\Phi_0^j\rangle\langle\Phi_0^j| \quad (3.4)$$

where Φ_0^j is the ground-state wave function of the harmonic oscillator with frequency, ω_j. The coherent state transform of the zero-temperature density operator for the harmonic bath and also the factor Λ entering the FBSD expression, are available analytically.[38] We set $\hat{A}_{\mathrm{mol}} = \hat{B}_{\mathrm{mol}} = \hat{\sigma}_z$ and $\hat{A}_{\mathrm{sol}} = \hat{B}_{\mathrm{sol}} = 1$ and report the TLS average position as a function of time, $\langle\sigma_z(t)\rangle$, at two values of the Kondo parameter.

The time-dependent TLS wave function is expressed as a linear combination of the orthogonal left- and right-localized basis functions

$$|\psi(t)\rangle = a_{\mathrm{L}}(t)|\varphi_{\mathrm{L}}\rangle + a_{\mathrm{R}}(t)|\varphi_{\mathrm{R}}\rangle \quad (3.5)$$

In the single-configuration approximation, the expansion coefficients are propagated in time according to the differential equations

$$i\hbar\dot{a}_{\mathrm{L}}(t) = \langle\varphi_{\mathrm{L}}|\hat{H}(t)|\varphi_{\mathrm{L}}\rangle a_{\mathrm{L}}(t) + \langle\varphi_{\mathrm{L}}|\hat{H}(t)|\varphi_{\mathrm{R}}\rangle a_{\mathrm{R}}(t) \quad (3.6)$$

$$i\hbar\dot{a}_{\mathrm{R}}(t) = \langle\varphi_{\mathrm{R}}|\hat{H}(t)|\varphi_{\mathrm{L}}\rangle a_{\mathrm{L}}(t) + \langle\varphi_{\mathrm{R}}|\hat{H}(t)|\varphi_{\mathrm{R}}\rangle a_{\mathrm{R}}(t) \quad (3.7)$$

where

$$\hat{H}(t) = -\hbar\Omega\hat{\sigma}_x + \sum_j \frac{1}{2}P_j(t)^2 + \sum_j \frac{1}{2}R_j(t)^2 - \hat{\sigma}_z\sum_j c_jR_j(t) \quad (3.8)$$

whereas the bath trajectories satisfy the differential equation

$$m\ddot{R}_j(t) = -m\omega_j{}^2R_j(t) + (|a_{\mathrm{R}}(t)|^2 - |a_{\mathrm{L}}(t)|^2)c_j \quad (3.9)$$

In the two-configuration calculation, the wave function is given again by eq 3.5, but the differential eqs 3.6 and 3.7 for the expansion coefficients now involve the Hamiltonian at two distinct trajectories, $\mathbf{R}^{(\mathrm{L})}$ and $\mathbf{R}^{(\mathrm{R})}$, which are now propagated according to the local force

$$m\ddot{R}_j^{\mathrm{L}}(t) = -m\omega_j{}^2R_j^{\mathrm{L}}(t) - c_j,\ \ m\ddot{R}_j^{\mathrm{R}}(t) = -m\omega_j{}^2R_j^{\mathrm{R}}(t) + c_j \quad (3.10)$$

In both cases, the expectation value of the TLS position

$$\langle\sigma_z(t)\rangle = |a_{\mathrm{R}}(t)|^2 - |a_{\mathrm{L}}(t)|^2 \quad (3.11)$$

is obtained by integrating eq 3.11 with respect to the bath trajectory initial conditions $\mathbf{R}_0$,$\mathbf{P}_0$.

Figure 1 shows the results of the quantum-FBSD calculations for two values of the Kondo parameter, $\xi = 0.09$ and 0.5675. Also shown are numerically exact results obtained via iterative evaluation of the path integral.[4] In the simplest single-configuration approximation, the results are very similar to those reported by Stock[72] using the quantum-classical approximation with a Wigner phase space density. As seen in Figure 1, the quantum-FBSD methodology reproduces the quenched tunneling oscillations semiquantitatively, predicting somewhat faster decoherence compared with the fully quantum mechanical results. This behavior is characteristic of FBSD (and other quasiclassical) methods and has been observed in similar calculations on single-minimum anharmonic oscillators.[26] Furthermore, Figure 1 shows that the two-configuration quantum-classical treatment significantly improves the agreement with the path integral results, leading to nearly exact results.

Unlike pure FBSD treatments, which fail to account for tunneling in a double-minimum potential, the mixed quantum-FBSD methodology is capable of capturing the tunneling effects over several tunneling oscillation periods. Therefore, the quantum-FBSD methodology corrects the main flaw of FBSD in cases where tunneling in real time is important.

IV. Concluding Remarks

We have shown that it is possible to extend the FBSD methodology to account for purely quantum mechanical effects along the dynamics, which cannot be captured by classical trajectories within a quasiclassical or semiclassical framework. In the quantum-FBSD methodology we introduced in this article, the time evolution is obtained through mixed quantum-classical propagation (which we have also extended to a multiconfiguration scheme), whereas the trajectory initial conditions are given by the coherent state matrix element prescribed in the FBSD methodology. Quantum-classical methods have been used extensively in the past, with either a fully classical or Wigner-type treatment of the density operator. The advantage of the present quantum-FBSD method arises from the simplicity of the coherent state transform that gives the FBSD phase space density, which can be evaluated on the fly by imaginary-time path integral methods, without having to resort to additional approximations. We have also presented a multiconfiguration

generalization of the quantum-classical propagation method that can be used in quantum-FBSD calculations.

Our numerical results on a prototype tunneling system coupled to a dissipative bath showed that the simple (single-configuration) quantum-FBSD scheme is able to account for quantum tunneling effects nearly quantitatively while maintaining the versatility of FBSD that is crucial to applications in complex many-particle environments. The somewhat more expensive two-configuration quantum-FBSD calculation led to almost perfect agreement with the numerically exact path integral results. Therefore, we envision that the quantum-FBSD methodology will allow the simulation of chemical processes such as proton and electron transfer in condensed phase or biological environments.

Acknowledgment. This material is based on work supported by the National Science Foundation under awards NSF CHE 05-18452 and CRIF 05-41659 and by the Donors of the Petroleum Research Fund under ACS PRF no. 42340-AC6.

References and Notes

(1) Metropolis, N.; Rosenbluth, A. W.; Rosenbluth, M. N.; Teller, H.; Teller, E. *J. Chem. Phys.* **1953**, *21*, 1087.
(2) Makri, N. *Comput. Phys. Commun.* **1991**, *63*, 389.
(3) Makri, N.; Makarov, D. E. *J. Chem. Phys.* **1995**, *102*, 4611.
(4) Makri, N.; Makarov, D. E. *J. Chem. Phys.* **1995**, *102*, 4600.
(5) Makri, N. *J. Math. Phys.* **1995**, *99*, 2430.
(6) Sim, E.; Makri, N. *Comput. Phys. Commun.* **1997**, *99*, 335.
(7) Makri, N. *J. Chem. Phys.* **1999**, *111*, 6164.
(8) Caldeira, A. O.; Leggett, A. J. *Physica A* **1983**, *121*, 587.
(9) Voth, G. A. *Adv. Chem. Phys.* **1996**, *93*, 135.
(10) Jang, S.; Voth, G. A. *J. Chem. Phys.* **1999**, *111*, 2371.
(11) Reichman, D. R.; Rabani, E. *Phys. Rev. Lett.* **2001**, *87*, 265702.
(12) Galliccio, E.; Berne, B. J. *J. Chem. Phys.* **1996**, *105*, 7064.
(13) Rabani, E.; Reichman, D. R.; Krilov, G.; Berne, B. J. *Proc. Natl. Acad Sci. U.S.A.* **2002**, *99*, 1129.
(14) Miller, T. F.; Manolopoulos, D. E. *J. Chem. Phys.* **2005**, *122*, 184503.
(15) Craig, I. R.; Manolopoulos, D. E. *J. Chem. Phys.* **2004**, *121*, 3368.
(16) Van Vleck, J. H. *Proc. Natl. Acad. Sci. U.S.A.* **1928**, *14*, 178.
(17) Miller, W. H. *J. Chem. Phys.* **1971**, *55*, 3146.
(18) Miller, W. H. *Adv. Chem. Phys.* **1975**, *30*, 77.
(19) Wang, H.; Thoss, M.; Sorge, K. L.; Gelabert, R.; Gimenez, X.; Miller, W. H. *J. Chem. Phys.* **2001**, *114*, 2562.
(20) Wigner, E. J. *Chem. Phys.* **1937**, *5*, 720.
(21) Wang, H.; Sun, X.; Miller, W. H. *J. Chem. Phys.* **1998**, *108*, 9726.
(22) Poulsen, J. A.; Nyman, G.; Rossky, P. J. *J. Chem. Phys.* **2003**, *119*, 12179.
(23) Makri, N.; Thompson, K. *Chem. Phys. Lett.* **1998**, *291*, 101.
(24) Thompson, K.; Makri, N. *J. Chem. Phys.* **1999**, *110*, 1343.
(25) Thompson, K.; Makri, N. *Phys. Rev. E* **1999**, *59*, R4729.
(26) Shao, J.; Makri, N. *J. Phys. Chem. A* **1999**, *103*, 7753.
(27) Shao, J.; Makri, N. *J. Phys. Chem. A* **1999**, *103*, 9479.
(28) Makri, N.; Nakayama, A.; Wright, N. *J. Theor. Comput. Chem.* **2004**, *3*, 391.
(29) Miller, W. H. *Faraday Discuss.* **1998**, *110*, 1.
(30) Sun, X.; Miller, W. H. *J. Chem. Phys.* **1999**, *110*, 6635.
(31) Skinner, D. E.; Miller, W. H. *J. Chem. Phys.* **1999**, *111*, 10787.
(32) Martin-Fierro, E.; Pollak, E. *J. Chem. Phys.* **2006**, *125*, 164104.
(33) Nakayama, A.; Makri, N. *J. Chem. Phys.* **2006**, *125*, 024503.
(34) Kegerreis, J.; Nakayama, A.; Makri, N. *J. Chem. Phys.* **2008**, *128*, 184509.
(35) Jadhao, V.; Makri, N. *J. Chem. Phys.* **2008**, *129*, 161102.
(36) Makri, N.; Shao, J. Semiclassical Time Evolution in the Forward-Backward Stationary-Phase Limit. In *Low-Lying Potential Energy Surfaces*; Hoffmann, M., Dyall, K. G., Eds.; ACS Symposium Series 828; American Chemical Society: Washington, DC, 2002; p 400.
(37) Jezek, E.; Makri, N. *J. Phys. Chem.* **2001**, *105*, 2851.
(38) Makri, N. *J. Phys. Chem. B* **2002**, *106*, 8390.
(39) Wright, N. J.; Makri, N. *J. Phys. Chem. B* **2004**, *108*, 6816.
(40) Nakayama, A.; Makri, N. *Chem. Phys.* **2004**, *304*, 147.
(41) Liu, J.; Makri, N. *Chem. Phys.* **2006**, *322*, 23.
(42) Liu, J.; Nakayama, A.; Makri, N. *Mol. Phys.* **2006**, *104*, 1267.
(43) Kegerreis, J.; Makri, N. *J. Comput. Chem.* **2007**, *28*, 818.
(44) Bukhman, E.; Makri, N. *J. Phys. Chem. A* **2007**, *111*, 11320.
(45) Chen, J.; Makri, N. *Mol. Phys.* **2008**, *106*, 443.
(46) Kuhn, O.; Makri, N. *J. Phys. Chem.* **1999**, *103*, 9487.
(47) Wright, N. J.; Makri, N. *J. Chem. Phys.* **2003**, *119*, 1634.
(48) Nakayama, A.; Makri, N. *J. Chem. Phys.* **2003**, *119*, 8592.
(49) Lawrence, C. P.; Nakayama, A.; Makri, N.; Skinner, J. L. *J. Chem. Phys.* **2004**, *120*, 6621.
(50) Nakayama, A.; Makri, N. *Proc. Natl. Acad. Sci. U.S.A.* **2005**, *102*, 4230.
(51) Haug, K.; Metiu, H. *J. Chem. Phys.* **1992**, *97*, 4781.
(52) Truong, T. N.; McCammon, J. A.; Kouri, D. J. *J. Chem. Phys.* **1992**, *96*, 8136.
(53) Shi, Q.; Geva, E. *J. Phys. Chem.* **2004**, *108*, 6109.
(54) Shi, Q.; Geva, E. *J. Chem. Phys.* **2004**, *121*, 3393.
(55) Bonella, S.; Coker, D. F. *Comput. Phys. Commun.* **2005**, *169*, 267.
(56) Heller, E. J. *J. Chem. Phys.* **1975**, *62*, 1544.
(57) Harris, R. *J. Chem. Phys.* **1980**, *72*, 1776.
(58) Gerber, R. B.; Buch, V.; Ratner, M. A. *J. Chem. Phys.* **1982**, *77*, 3022.
(59) Buch, V.; Gerber, R. B.; Ratner, M. A. *Chem. Phys. Lett.* **1983**, *101*, 44.
(60) Gerber, R. B.; Ratner, M. A. *Adv. Chem. Phys.* **1988**, *70*, 97.
(61) Schatz, G. C.; Buch, V.; Ratner, M. A.; Gerber, R. B. *J. Chem. Phys.* **1983**, *79*, 1808.
(62) Leggett, A. J.; Chakravarty, S.; Dorsey, A. T.; Fisher, M. P. A.; Garg, A.; Zwerger, M. *Rev. Mod. Phys.* **1987**, *59*, 1.
(63) Feynman, R. P. *Rev. Mod. Phys.* **1948**, *20*, 367.
(64) Feynman, R. P.; Hibbs, A. R. *Quantum Mechanics and Path Integrals*; McGraw-Hill: New York, 1965.
(65) Feynman, R. P. *Statistical Mechanics*; Addison-Wesley: Redwood City, CA, 1972.
(66) Glauber, R. J. *Phys. Rev.* **1963**, *130*, 2529.
(67) Shi, Q.; Geva, E. *J. Phys. Chem. A* **2003**, *107*, 9059.
(68) Liu, J.; Miller, W. H. *J. Chem. Phys.* **2006**, *125*, 224104.
(69) Makri, N.; Miller, W. H. *J. Chem. Phys.* **1987**, *87*, 5781.
(70) Meyer, H.-D.; Manthe, U.; Cederbaum, L. S. *Chem. Phys. Lett.* **1990**, *165*, 73.
(71) Makri, N. *J. Phys. Chem.* **1999**, *103*, 2823.
(72) Stock, G. *J. Chem. Phys.* **1995**, *103*, 1561.

JP809741X